Fragility assessment of chemical storage tanks subject to floods

Khakzad, N.; van Gelder, Pieter

DOI
10.1016/j.psep.2017.06.012

Publication date
2017

Document Version
Accepted author manuscript

Published in
Process Safety and Environmental Protection

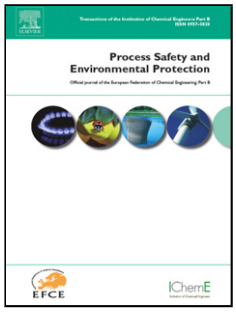

Title: Fragility assessment of chemical storage tanks subject to floods

Authors: Nima Khakzad, Pieter Van Gelder

PII: S0957-5820(17)30193-3
DOI: http://dx.doi.org/doi:10.1016/j.psep.2017.06.012
Reference: PSEP 1093

To appear in: *Process Safety and Environment Protection*

Received date: 19-4-2017
Revised date: 12-6-2017
Accepted date: 19-6-2017

Please cite this article as: Khakzad, Nima, Gelder, Pieter Van, Fragility assessment of chemical storage tanks subject to floods.Process Safety and Environment Protection http://dx.doi.org/10.1016/j.psep.2017.06.012

Fragility assessment of chemical storage tanks subject to floods

Nima Khakzad*, Pieter Van Gelder

Safety and Security Science Group, TU Delft, The Netherlands

Corresponding author: n.khakzadrostami@tudelft.nl
Phone: +31 15 27 84709

Highlights

- A methodology is proposed for fragility assessment of chemical plants in case of floods.
- Fragility functions are generated using limit state equations and logistic regression.
- Floatation, shell buckling, and impact-induced sliding are considered as prevailing failure modes.
- Bayesian network is used to combine the fragility functions
-

Abstract

In the context of natural-technological (natech) accidents, flood-induced damage of chemical facilities have received relatively less attention mainly due to the scarcity of experimental or high resolution field observations. In the present study, we have introduced a methodology based on load-resistance relationships to assess the vulnerability of process facilities in form of fragility functions. While logistic regression is used to develop fragility functions for different failure modes such as floatation, buckling, and sliding, Bayesian network is employed to combine the fragility functions, taking into account common causes and conditional dependencies. Although the application of the methodology has been demonstrated on atmospheric storage tanks, it can be applied to fragility assessment of a variety of chemical and process vessels.

Keywords: Natech accidents; Floods; Atmospheric storage tanks; Logistic regression; Bayesian network.

1. Introduction

Technological accidents which are triggered by natural events such as earthquakes, hurricanes, floods, and lightings, are known as natech (natural-technological) accidents. The occurrence of natech accidents in chemical and process plants, particularly, can pose disastrous risks to human and the environment due to the release and spread of toxic and flammable chemicals in large quantities. Compared to safety accidents, which are usually a matter of equipment failure or human error, natech accidents can lead to more severe consequences as from one side they can cause multiple and simultaneous failures of process vessels which in turn can lead to domino effects, and from the other side they can damage infrastructures (e.g., power grids, communication networks, water distribution systems, transportation networks, etc.) required for conducting a timely and effective emergency response (Campedel, 2008; Krausmann and Mushtaq, 2008).

To account for the risk of natech accidents in the quantitative risk assessment of chemical facilities, the correlation between the parameters of a natural event (e.g., the frequency and the peak gravitational acceleration of an earthquake) and the observed damage states of impacted vessels should be identified; the result is usually displayed in form of fragility curves, where the parameter of interest (or a polynomial function of the parameters of interest) and the (cumulative) probability of damage are presented on the abscissa and ordinate axes, respectively (Salzano et al., 2003; Korkmazet al., 2011; Girgin and Krausmann, 2013).

As opposed to the natech accidents in chemical plants which have been caused by earthquakes or storms (high winds), the ones triggered by floods have received less attention (Campedel, 2008), both in the relevant design standards and regulations (API 620, 2013; API 650, 2007; ASCE-7, 2006; FEMA, 1995) and available literature. This has mainly been due to the rarity of flood-induced natech accidents in general – constituting only 2 to 4% of industrial accidents (Cozzani et al., 2010) – and partly due to the scarcity of historical or experimental data relating the characteristics of floods (frequency of flood, water height, water speed) to the damage states (or failure mode) of impacted equipment. As pointed out by Campedel (2008), only for a limited number of floods the height of flood inundation have been identified (e.g., see Santella et al., 2010) whereas there are even a lesser number of floods with known water speed. Aside from the lack of detailed data about the floods' characteristics, the available information in the literature about the failure modes and the cause of chemical release is usually qualitative (Godoy, 2007; Campedel, 2008; Krausmann and Mushtaq, 2008; Santella et al., 2010), not determining the severity of damage. Further, in most

cases, for example, it is not clarified if the chemical release has been due to disconnected pipelines or the structural collapse of the vessel (Cozzani et al., 2010).

Investigating a number of major accident databases throughout Europe and the U.S., Cozzani et al. (2010) identified, based on 272 flood-induced natech accidents from 1960 to 2007, the aboveground storage tanks as the most frequently damaged equipment (74% of cases), including atmospheric storage tanks, floating roof tanks, and pressurized tanks, in a descending order. Besides, the displacement of equipment (due to rigid sliding or floating), shell rupture due to impact with debris, and the collapse of equipment (it has not been defined whether due to overturning or shell buckling) have been identified as the prevailing failure modes (Cozzani et al., 2010). Similar failure modes have been reported in Godoy (2007) based on the site observations of affected process plants in Louisiana and Texas, U.S., following Hurricane Katrina in 2005, where the buckling of tanks' shell was mainly attributed with the strong winds not the ensuing flood[1]. It is also worth mentioning that the pipeline disconnection as a lateral failure mode resulting from the displacement of equipment has reportedly led to significant chemical releases as well (Godoy, 2007; Campedel, 2008; Cozzani et al., 2010).

Due to the scarcity of historical data with sufficient resolution, the majority of previous quantitative risk assessment studies has relied on analytical or numerical techniques to calculate the probability of failure (modes) based on the failure mechanism (physics of failure) of impacted vessels (Landucci et al., 2012, 2014; Mebarki et al., 2014; Kameshwar and Padgett, 2015). In almost all previous studies, based on a comparison between the flood-induced forces (loads) exerted on a vessel (e.g., buoyant force of water) and the resistance of the vessel (e.g., weight of the vessel and its contents), limit state equations (LSEs) have been developed for different failure modes of the vessel. Using the LSEs, either the critical values of influential parameters, e.g., the critical height of liquid inside the storage tank to prevent from buckling of the tank shell, have been determined (Landucci et al., 2012, 2014) or assuming probability distributions for random load-resistance parameters, a number of fragility curves have been developed to correlate the load-resistance parameters to failure probabilities (Mebarki et al., 2014). In a slightly different approach, Kameshwar and Padgett (2015) used LSEs in conjunction with Latin hypercube sampling to generate data required for logistic regression.

In the abovementioned studies, however, the focus has been on a few failure modes and not necessarily the most credible ones (e.g., Landucci et al., 2012). And where more than one failure

[1] Hurricane Katrina caused the levees along the Mississippi River to breach, leading to the inundation of process plants in the floodplains beyond the levees (Godoy, 2007).

mode have been investigated (Mebarki et al., 2014; Kameshwar and Padgett, 2015), the resulting fragility functions have been combined deterministically, assuming independent failure modes. This latter oversimplification, however, can significantly compromise the reliability of end results since the same flood-induced loads contribute to all the failure modes of an impacted vessel, making the failure modes and thus the fragility functions heavily correlated.

Bayesian network (BN) is a probabilistic graphical technique (Pearl, 1988; Neapolitan, 2003) with an ample potential in modeling and reasoning of complex systems where conditional dependencies are predominant. BN has been employed as a promising tool to tackle data scarcity where both objective data (through observation, inspection, monitoring, etc.) and subjective data (elicited from subject matter experts) can be combined for reasoning and accounting for both aleatory and epistemic uncertainties (Khakzad et al., 2011). The belief updating feature of BN further makes it possible to reduce data uncertainty through probability updating and adapting (Khakzad et al., 2013) as new information becomes available. Although BN has widely been used in process safety and risk management, its application to fragility assessment of natech accidents has been very limited, if any.

The present study is aimed at presenting a structured methodology based on previous studies to develop and combine fragility functions for a broader range of flood-induced failure modes. The schematic of the proposed methodology has been illustrated in Figure 1 while the steps taken will be addressed in more detail in the following sections. In Section 2, the failure modes of aboveground atmospheric storage tanks (hereafter, storage tanks) will be modeled using LSEs (Steps 1-3 in Figure 1). These equations will be coupled with Monte Carlo simulation to generate data required to develop fragility functions using logistic regression (Steps 4-6 in Figure 1). In Sections 3 and 4, the basics of logistic regression (used in Steps 7 and 8 in Figure 1)and BN (used in Steps 9 and 10 in Figure 1) will be recapitulated, respectively. The application of the methodology will be demonstrated in Section 5 for aboveground atmospheric storage tanks as a type of equipment having experienced most of failure modes (Godoy, 2007; Krausmann and Mushtaq, 2008; Cozzani et al., 2010).The conclusions are presented in Section 6.

2. Failure modes: limit state equations

2.1. Floatation

Displacement of storage tanks mainly due to floatation has reportedly been the most frequent flood-induced failure mode according to the observations made after the Hurricane Katrina (Godoy,

2007; Santella et al., 2010) and the investigation of major accident databases (Cozzani et al., 2010). As reported by Godoy (2007), displacements of up to 30 m have been recorded due to the flood subsequent to the Hurricane Katrina, causing either pipeline detachment or severe structural damages.

To develop the LSE representing the floatation of a storage tank, the main resisting forces, which are the weight of the tank bulk W_T and the weight of the contained chemical W_L, and the loading force, which is the buoyant force F_B of flood (White, 2003), have been denoted on a typical storage tank in Figure 2, where D, H, and tare the tank's diameter, height, and thickness. The height of the chemical inside the tank and the water inundation have been denoted, respectively, by h and S. Although the specifications for the anchorage of storage tanks have been given in current standards (e.g., API, 650), the common design practice in many plants is still based on self-anchored storage tanks (Godoy, 2007). Depending on whether the tank is anchored or not, a resisting force F_F provided by the anchorage system (e.g., bolts and the concrete foundation) should also be considered (Kameshwar and Padgett, 2015).

Considering the direction of the loading and resisting forces in Figure 2, the floatation limit state equation, $LSE_{Floatation}$, can be developed in Equations (1)-(4):

$$LSE_{Floatation} = F_B - W_T - W_L \quad (1)$$

$$F_B = \rho_w g \frac{\pi D^2}{4} S \quad (2)$$

$$W_T = \rho_s g \left(\pi DH + 2\frac{\pi D^2}{4}\right) t \quad (3)$$

$$W_L = \rho_l g \frac{\pi D^2}{4} h \quad (4)$$

where ρ_w, ρ_s, and ρ_l are the densities $(\frac{kg}{m^3})$ of the flood water, tank shell (usually steel), and the chemical substance inside the tank, respectively; $g = 9.81\frac{m}{S^2}$ is gravitational acceleration. Equation (1) can further be extended to account for the resistance force of foundation (e.g., tensile stress of bolts and the concrete slab) in case of anchored process vessels. (Kameshwar and Padgett, 2015). As can be seen from Equation (1), the tank will float if $LSE_{Floatation} > 0$. It is also worth noting that the only flood parameter contributing to this failure mode is the height of flood inundation, S.

2.2. Shell buckling

As reported by Godoy (2007), the shell buckling of storage tanks was mainly caused by high winds during the Hurricanes Katrina and Rita rather than by the subsequent flood (in case of Katrina). However, Campedel (2008) and Cozzani et al. (2010) have pointed out the shell buckling as a potential failure mode[2], where an external pressure above the critical pressure P_{cr} leads to the shell collapse.

To develop the LSE of the shell buckling, the main internal (resisting) and external (loading) radial pressures on the shell have been depicted in Figure 3. These radial pressures include the hydrostatic pressure both from the height of liquid inside the tank P_L and from the height of flood inundationP_s and the hydrodynamic pressure P_d due to the kinetic energy (speed) of the flood flow. Accordingly, the LSE for shell buckling can be developed as Equation (5). The amounts of hydrostatic pressures P_L and P_s which increase linearly with depth (white, 2003) have been presented in Equations (6) and (7) for the maximum values at the bottom of the tank. As a result, Equation (5) presents the buckling condition at the base of the storage tank. To model the hydrodynamic pressure, a uniform distribution can be considered along the water inundation column (ASCE/SEI 7-05, 2006) as presented in Equation (8).

$$LSE_{Buckling} = P_s + P_d - P_L - P_{cr} \quad (5)$$

$$P_L = \rho_l g h \quad (6)$$

$$P_s = \rho_w g S \quad (7)$$

$$P_d = \frac{1}{2} C_d \rho_w V^2 \quad (8)$$

where C_d is the drag coefficient (C_d = 2.0 for square and rectangular piles, and C_d = 1.2 for round piles); V is the average speed of the flow ($\frac{m}{S}$). For cylindrical shell structures which are subject to radial pressure, the amount of buckling critical pressure P_{cr}(Pa) can be calculated using simplified relationships given in Equation (9) for long cylinders (Iturgaiz Elso, 2012) and in Equation (10) for short cylinders (Landucci et al., 2012), respectively.

$$P_{cr} = \frac{E}{1-v^2} (\frac{t}{D})^3 \quad (9)$$

[2] Actually Cozzani et al. (2010) did not explicitly mention the shell buckling as a failure mode but referred to it via "collapse for instability."

$$P_{cr} = \frac{2Et}{D}\left\{\frac{1}{(n^2-1)\left[1+\left(\frac{2nH}{\pi D}\right)^2\right]^2} + \frac{t^2}{3(1-v^2)D^2}\left[n^2 - 1 + \frac{2n^2-1-v}{\left(\frac{2nH}{\pi D}\right)^2-1}\right]\right\} \text{ for } n \geq 2 \quad (10)$$

where E is the Young's modulus of the tank material (Pa); v is Poisson ratio; n is the number of waves involved in buckling. As can be seen from Equation (5), the tank shell will buckle if $LSE_{Buckling} > 0$, indicating the net pressure on the shell is beyond the critical threshold. It is also worth noting that the flood parameters S and V both contribute to the buckling failure mode.

2.3. Rigid sliding

As for unanchored storage tanks, the rigid sliding due to the hydrodynamic pressure of the flood surge has been reported as a potential failure mode in Cozzani et al. (2010). Further, as pointed out by Mebarki et al. (2014), both large and small size storage tanks are vulnerable to sliding; for small size storage tanks, sliding is even likelier to cause more severe damages than buckling and floatation (perhaps due to the detachment of connected pipelines).

To develop the LSE of sliding, considering the storage tank and its containment as a body of mass, the hydrodynamic force of the flood (load) and the friction force between the tank and the ground (resistance) are taken into account in Equation (11). Accordingly, the hydrodynamic force F_d can be calculated as the product of the hydrodynamic pressure P_d and the vertical wet section area of the storage tank, D×S, as shown in Equation (12). The friction force F_{fr} is equal to the product of the friction coefficient C_f and the normal force F_N exerted from the ground to the bottom of the tank, as shown in Equation (13). For an unanchored storage tank, the normal force is the vector summation of the weight of the tank and its containment and the buoyant force, as shown in Equation (14), yet inasmuch as the tank is not floated (i.e., $F_N \geq 0$). Having the load, F_d, and the resistance, F_{fr}, the LSE for sliding can be developed as in Equation (11), where $LSE_{Sliding} > 0$ indicates the failure of the tank. As can be noted, both flood parameters S and V contribute to the sliding failure mode.

$$LSE_{Sliding} = F_d - F_{fr} \quad (11)$$

$$F_d = P_d DS \quad (12)$$

$$F_{fr} = C_f F_N \quad (13)$$

$$F_N = W_T + W_L - F_B \quad (14)$$

where C_f is the friction coefficient (0.4 according to API 650). It should be noted that according to the stationary modeling of the load-resistance forces, the hydrostatic force would not seem to play a role in sliding. This is because the same amount of water inundation height and thus equal

amount of hydrostatic force would exist on the other side (downstream) of the storage tank. It should be noted that the existence of the friction force is legitimate as long as the tank stays in touch with the ground; in other words, if the floatation failure mode occurs first, the sliding failure mode will be excluded from the analysis. Such conditional dependency (negative correlation) should be taken into account when integrating these failure modes.

2.4. Impact of debris

Impact with waterborne debris and especially with other floating storage tanks is reportedly among the failure modes leading to severe damages (Krausmann and Mushtaq, 2008; Cozzani et al., 2010; Mebarki et al., 2014).Predicting the magnitude of the impact force and the force's point of action is very challenging and subject to many uncertain parameters. Following the impulse-momentum approach, the time-averaged impact force (Haehnel and Daly, 2004) can be calculated from Equation (15):

$$F_i = \frac{MU}{t_i} \tag{15}$$

where M is the debris mass (kg); U is the debris velocity ($\frac{m}{s}$), usually assumed equal to V; t_i is the impact duration (s), measured from the moment of contact until the impact forces reaches its maximum value. ASCE-7 (2006) has adopted a value of t_i =0.03s. To consider differences between the flood velocity V and the velocity of large debris U, ASCE-7 (2006) suggested a modified impact force relationship as shown in Equation (16):

$$F_i = \frac{MUC_O C_D C_B}{t_i} \tag{16}$$

where C_O is the orientation coefficient (equal to 0.8) to account for eccentric impacts; C_D is the depth coefficient to account for the debris' velocity reduction due to possible dragging along the bottom, varying from 0.0 to 1.0 for a height of flood inundation, S, between 0.3m and 1.5m, respectively[3]; and C_B is the blockage coefficient to account for the debris' velocity reduction due to prior collisions with other obstacles, varying from 0.0 to 1.0 for flow a flood width, W, between 1.5m and 9.0m, respectively[4].

Based on experimental data, Haehnel and Daly (2004) also suggested Equation (17) for the impact force of woody debris of different mass and velocity:

$$F_i = 1550U\sqrt{M} \tag{17}$$

[3] C_D= 0.0 if S ≤ 0.3m; C_D=0.833 (S-0.3) if 0.3 < S ≤ 1.5; C_D= 1.0 if S > 1.5m.
[4] C_B= 0.0 if W ≤ 1.5m; C_B= 0.133 (W-1.5) if 1.5 < W ≤ 9.0; C_B= 1.0 if W > 9.0 m.

For design purposes, as suggested by ASCE-7 (2006), the normal impact forces such as those inflicted by woody debris (e.g., tree logs) can be considered as a point force acting horizontally at the flood elevation on a 0.09 m^2 surface of the target. As for special impact forces, that is, forces incurred by large objects such as broken up ice floats and accumulations of debris, in absence of a detailed analysis, a uniform load of 1.48 kN/m acting over a 0.31 m high horizontal strip at the flood elevation can be considered. Regarding the extreme impacts forces, i.e., those incurred by very large objects, such as boats, barges, or collapsed buildings, no guidelines have been recommended.

Since the impact force of floating storage tanks in a chemical facility can be categorized as special or extreme impact forces, depending on the size of the tank, we suggest such impact forces be taken into account in one of the following ways:

(i) the impact force can be added to Equation (11) when considering the sliding of the impacted storage tank;

(ii) the impact force (after converted to stress)can be added to Equation (5) when considering the shell buckling of the impacted storage tank; or

(iii) a new LSE can be developed to determine whether the impact force exceeds the critical shear stress $\sigma_{cr}$of the shell, leading to the rupture of the tank shell.

3. Logistic regression

Considering a Bernoulli experiment with a binary output variable as Y (0,1), the binomial logistic regression can be used to predict the outcome of the experiment using a probability function$P(x) = P(Y = 1|X = x)$where X can be a set of parameters (covariates). Having the logistic transformation (or logit) of $P(x)$ as a linear function of x as$ln\frac{P(x)}{1-P(x)} = \beta_0 + \beta_1 x$, the probability function can be presented in Equation (18):

$$P(x) = \frac{e^{\Psi(x)}}{1+e^{\Psi(x)}} \tag{18}$$

where $\Psi(x) = \beta_0 + \beta_1 x$ is the logit function, and β_0 and β_1 are the parameters of the logistic regression, which can be estimated by maximizing the likelihood function of $P(x)$given an observation of the experiment outcome, as shown by Hosmer et al. (2013) and Van Erp and Van Gelder (2013) using a Bayesian inference scheme. Assuming a Bernoulli experiment (Y=1if the storage tank fails and Y=0if the tank does not fail) with a probability distribution of $P(x)$, the likelihood function for n observations can be developed as Equation (19):

$$Likelihood = \prod_{i=1}^{n} P(Y = y_i|X = x_i) = \prod_{i=1}^{n} P(x_i)^{y_i}(1 - P(x_i))^{1-y_i} \quad (19)$$

For the sake of computational simplicity, the natural logarithm of the likelihood function, known as log-likelihood, can be maximized instead of the likelihood function.

4. Bayesian network

Bayesian network (BN)is a graphical technique for reasoning under uncertainty (Pearl, 1988). In a BN, a system's random variables are represented by chance nodes while the conditional dependencies among the variables are represented using arcs, usually drawn from causes to the effects. The nodes with arcs directed from them are called parent nodes while the ones with arcs directed into them are called child nodes. Further, the nodes with no parent (e.g., X1 in Figure 4) are known as root nodes, the nodes with no children (e.g., X3 and X4 in Figure 4) are called leaf nodes, and the other nodes (e.g., X2 in Figure 4) are called intermediate nodes. The type of cause-effect relationships among the connected nodes are encoded in form of conditional probabilities assigned to the nodes except the root nodes which are identified by marginal probabilities.

Considering the local dependencies and the chain rule, the joint probability distribution of the random variable presented in the BN can be factorized as the multiplication of marginal and conditional probabilities. For example, according to the BN in Figure 4, $P(X1, X2, X3, X4) = P(X1)P(X2|X1)P(X3|X1, X2)P(X4|X2)$. BN can be used for either forward reasoning, where, for example, the knowledge about X1 can be used to deduce about X4, or backward reasoning, in which via employing the Bayes' rule, an observation about X4 can be used to infer about X1. The main advantages of BN over conventional techniques such as fault tree analysis are its capability of considering conditional dependencies, handling multistate variables, and applying Bayes' rule for belief updating (backward reasoning) (Khakzad et al., 2011).

5. An illustrative example

5.1. Case study

To illustrate the application of the developed methodology to fragility assessment of chemical atmospheric storage tanks, consider two unanchored storage tanks in Figure 5, Tank 1 and Tank 2, each with a capacity of 40,000 m^3, diameter of D= 91.5 m, height of H= 6.1 m, and shell thickness of t= 15 mm, used to store crude oil.

The tanks' specifications are the standard dimensions of atmospheric storage tanks according to API 650. The reason for the selection of tanks with such dimensions is to make the case study as similar as possible to the storage tanks reported in Godoy (2007), in which an unanchored 40,000-m^3storage tank which was filled to 25% of its capacity (i.e., h= 1.57 m) with crude oil floated subject to a flood inundation height of 3.7 m after the Hurricane Katrina.

For flood-induced fragility assessment of storage tanks, a comprehensive flood hazard assessment should be performed to identify the frequency of floods along with parameters such as the height of inundation, S, and flow velocity, V. This demands for a thorough investigation of mechanisms that can lead to floods, including extreme precipitation, snow melting, and dam breaks, along with the hydrological and topological aspects of floodplains (van Gelder, 2013), which are beyond the scope of the present study. Investigating the historical flood-induced damages in chemical and process facilities, Campedel (2008) determined three types of floods: (i) high water condition, where S > 1m and V= 0.25m/s, (ii) high flow condition, where V > 2 m/s and S= 0.5m, and (iii) high risk condition, where S= 1m and V= 1m/s. Accordingly, in the present study, for illustrative purposes, three types of flood are considered:

- Flood 1[5]: S= 3.7m, V= 0.25m/s
- Flood 2: S= 0.5m, V= 2.5m/s
- Flood 3: S= 1m, V= 1m/s

5.2. Results

5.2.1. Floatation fragility assessment

To derive the floatation fragility curves of Tank 1 exposed to the aforementioned floods, Monte Carlo simulation was used to generate random values of $LSE_{Floatation}$ as in Equation (1). For illustrative purposes only, all the parameters were assumed constant (Table 1) whereas the height of crude oil inside the tank which was considered to follow a uniform distribution h1 ~ Uniform (0.0, 5.2). Since h1 is the only random variable playing a role in the LSE, we, for illustrative purposes, limited the number of Monte Carlo simulations to 2000.

In this regard, the positive values of $LSE_{Floatation}$ was considered as an indication of the tank floatation, Y= 1.0, whereas negative values were considered as the tank not being floated, Y= 0.0.

[5] S has deliberately been assumed 3.7 m so as to simulate the damage condition of the storage tank reported in Godoy (2007).

Corresponding to each random value of h1 (and thus a random value of $LSE_{Floatation}$), a floatation probability P(h1) was predicted using Equation (18) for arbitrarily initial values of β_0 and β_1 (both equal to 0.5 in this study). Forming a likelihood function for each set of h1, Y, and P(h1) using Equation (19), the optimal values of β_0 and β_1 were estimated using the maximum likelihood estimation analysis. The floatation fragility curves of Tank 1 due to the floods are depicted in Figure 6 while the optimal values of regression parameters being listed in Table 2.

As reported in Godoy (2007), a storage tank with the same dimensions as of Tank 1and filled with h1= 1.57m of crude oil, was seen to float when exposed to a flood inundation height of approximately 3.7m. This observation has been denoted in Figure 6 with a vertical dotted line for which the probability of floatation in case of Flood 1 (S= 3.7 m) is equal to 1.0. It is also worth noting that in Figure 6, during each flood, the critical height of crude oil inside the storage tank – the height below which the tank becomes floated, i.e., P(h1)= 0.5 – is roughly equal to the flood inundation height, S. This is in agreement with the recommendations in Flood Preparedness Factsheet (RRT6, 2016), where the minimum height of chemical content to avoid the floatation has been proposed equal to the height of flood inundation.

5.2.2. Buckling fragility assessment

Following the same procedure, Equations (5)-(8) and (10) can be used to generate random values of $LSE_{Buckling}$ given the flood inundation heights and flow velocities of the floods. The developed fragility curve of Tank 1 due to shell buckling has been depicted in Figure 7 only for Flood 1 since the other floods do not result in the shell buckling. As can be noted from Figure 7, the flood inundation height seems to play the key role in shell buckling since among the three floods only the one with a considerable inundation height (Flood 1 with S= 3.7m) could result in shell buckling. Such result is in compliance with the observations in Campedel (2008), where high water levels have been attributed to shell instability of atmospheric tanks while high water speeds have been blamed for the failure of the support structures of pressurized tanks. Moreover, as can be seen in Figure 8, the high-water Flood 1 can result in shell buckling given that the height of crude oil inside the tank is quite low ($h \leq 0.6$m). In other words, the higher height of chemical content helps

significantly reduce the probability of shell buckling, as has been reported in (RRT6, 2016). The optimal values of regression parameters are listed in Table 2.

5.2.3. Sliding fragility assessment

As for sliding failure mode, none of the floods could result in the sliding of Tank 1. This is owing to the fact that:(i) for high-water floods (especially Flood 1) the tank becomes floated before the hydrodynamic force of flood P_d finds a chance to cause the tank to slide;(ii) for high-flow floods (especially Flood 2), however, the buoyancy force F_B is not large enough to decrease the normal force F_N and subsequently the friction force F_{fr} to a sufficiently low amount so as to let P_d slide the tank. For the sake of clarity, the sliding fragility curve of Tank 1 in case of an imaginary extreme flood with S= 1.0m and V= 20m/s has been displayed in Figure 8. As can be seen, even for such an unlikely extreme flood, the probability of sliding is only credible for a limited range of crude oil's height inside the tank, $0.84 \leq h \leq 2.84$. As can be noted, for $h < 0.84$ the tank will float (this has been denoted by a vertical dashed line in Figure 8) whereas for $h > 2.84$ the friction force exceeds (due to the increased bulk weight of the tank) the hydrodynamic force and thus no sliding.

5.2.4. Impact fragility assessment

Due to the uncertainties involved in the calculation of impact-induced shell buckling or shell rupture failure modes, in the present study, the impact force is merely considered as a propulsive force contributing to the sliding of an impacted storage tank. To this end, given that Tank 1 in Figure 6 both floats (see the floatation regression parameters of Tank 1 in Table 2) and collides with Tank 2, the impact force of Tank 1 has been calculated using Equation (15) and added to Equation (11) to account for the $LSE_{Sliding}$ of Tank 2.

Since the magnitude of the impact force is a function of the height of crude oil, h1, inside Tank 1 (via M in Equation (15)), and the magnitude of the friction force depends on the height of crude oil, h2, inside Tank 2 (via W_L in Equation (14)), a multivariable logit function was developed to estimate the conditional probability of sliding of Tank 2 as $\Psi(h1,h2)=\beta_0+\beta_1 h1+ \beta_2 h2$. The optimal values of the regression parameters are listed in Table 2 under Tank 2. As can be noted from Table 2, unlike Tank 1, sliding is a possible failure mode for Tank 2, even without being exposed to an extreme

flood which is the case in Figure 8; this highlights the significant role of impact forces in failure mode analysis of storage tanks during floods.

The conditional sliding probability of Tank 2 given that Tank 1 floats and Tank 2 does not float should be considered when combining the failure modes using the BN in the next section (see the arcs from "Floating Tank 1" and "Floating Tank 2" to "Sliding Tank 2" in Figure 9).

5.2.5. Combination of failure modes

Calculating individual fragility functions in the previous sections, a BN can be employed to combine the failure probabilities (Figure 9), in which the node "Flood" have three states as Flood 1, Flood 2, and Flood 3 while the nodes "h1" and "h2" have discrete states ranging from 0.0 to 5.2m. Having the characteristics of the floods, i.e., S and V, and the states of h1 and h2, the probabilities of floating, buckling, and sliding[6] can be estimated for the storage tanks using the regression parameters listed in Table 2. We, for illustrative purposes, instantiated the node "Flood" to the state Flood 1 due to the contribution of Flood 1 to most of failure modes (see Table 2). For the sake of better clarity, the parts of BN allotted to the failure analysis of Tank 1 and Tank 2 have been identified using solid and dashed lines, respectively.

As previously mentioned (see Section 2.3), if a tank floats, the sliding will no longer be considered as a failure mode thereof. To take into account such conditional dependency between these two failure modes, as for Tank 1, for instance, there is an arc from "Floating Tank 1" to "Sliding Tank 1" in Figure 9, accounting for P(Tank 1 slides | Tank 1 floats) = 0.0.

As for Tank 2, in addition to the forgoing dependency between the same tank's floating and sliding modes (the arc from "Floating Tank 2" to "Sliding Tank 2"), there is an arc from "Floating Tank 1" to "Sliding Tank 2" to account for the impact-induced sliding of Tank 2 given the floatation of Tank 1, that is, P(Tank 2 slides | Tank 1 does not float) =0.0. Likewise, there are arcs from both h1 and h2 to "Sliding Tank 2" since the respective logistic regression is a function of both variables, that is, $\Psi(h1,h2)=\beta_0+\beta_1 h1+ \beta_2 h2$.

The total failure probability of each tank can be calculated as the union of single failure modes as P(Failure)= P(Floating ∪ Buckling ∪ Sliding) while considering the dependencies arising from

[6] Although Tank 1 does not slide, the node "Sliding Tank 1" has been presented in the BN for the sake of clarity.

common causes (load-resistance parameters) and conditional cause-effect relationships. Regarding Tank 2, for instance, the individual and total failure probabilities in case of Flood 1 are calculated as P(Floating)= 0.72, P(Buckling)= 0.33, P(Sliding)= 0.139, and P(Failure)= 0.859, considering discrete states of h1 and h2, where $0.0 \leq hi \leq 5.2$ for i= 1, 2.

Using the BN in Figure 9, the total failure probability of each tank can be calculated for discretized states of respective h, resulting in total fragility curves. Figure 10 illustrates the individual and total fragility curves of Tank 2 calculated by modeling the BN in GeNIe (2014). Since for Tank 2 the probability of impact-induced sliding is a function of both h1 and h2, in order to display the two-dimensional fragility curve in Figure 10, the probability of impact-induced sliding has been averaged over h1.

As can be noted from Figure 10, up to $h2 \sim 3.7$m the floating of Tank 2 is the predominant failure mode whereas from this point on the sliding failure mode is more probable; accordingly, the least failure probability of the tank and thus the most stable condition is associated with $h2 \sim 4.1$m.

5.3 Discussion

In the previous sections we illustrated how load-resistance relationships and Monte Carlo simulation can be used to generate data required for the development of fragility functions for flood-induced failure modes of atmospheric storage tanks. It was also demonstrated how a BN can be developed to combine the individual failure modes to render a total fragility function while considering the common causes and conditional dependencies. The present study was aimed at introducing a methodology for vulnerability assessment of chemical/process installations in the context of natech accidents; as such, the effort was mainly devoted to the construction of a practicable framework based on simplifying assumptions and conventional techniques, merely for illustrative purposes.

Nevertheless, one can readily improve the reliability and accuracy of the developed methodology by applying more sophisticated techniques and state-of-the-art tools. In this regard, the efficacy of the developed methodology may be increased via application of numerical simulations such as finite difference method for shallow water equations, computational fluid dynamics, and finite element method to model the flood propagation as well as the dynamic impact of the flood front on the process vessels. Numerical simulations can particularly be helpful in dealing with complicated failure modes such as impact-induced shell buckling or shell rupture, where a three-dimensional simulation of load-resistance forces would result in a better understanding of failure mechanisms.

For instance, the simplifying assumption of constant hydrodynamic pressure distribution in Figure 3 cannot seem to be accurate for storage tanks of large diameter as the magnitude of the hydrodynamic pressure will vary along the circumference of the tank. This pressure distribution can affect the buckling response of storage tanks under external loads. However, it is worth mentioning that in the context of quantitative risk assessment of chemical plants, one might have to deal with a large number of vessels of different type and dimension a detailed failure analysis of which would be very costly. This latter constraint imposed by the large number and diversity of process vessels in a typical process plant, however, may justify the application of stationary modeling of flood-structure interaction.

Other issues worth considering in future work would be the inclusion of other failure modes such as capsizing (overturning) and impact-induced rupture and buckling, and also the treatment of more parameters as random variables (we only considered the height of chemical containment as a random variable), and application of more sophisticated regression techniques such as Bayesian regression (Van Erp and Van Gelder, 2013). Regarding the former issue, this simplifying assumption of constant parameters such as the shell thickness or the height of inundation does not seem to limit the application of the developed methodology since the uncertainty in the estimation of such random variables can readily be modeled via appropriate probability distributions. As for the latter issue, however, a Bayesian regression technique not only can facilitate the development of fragility functions with a lesser amount of data, which is dominant in flood-induced natech accidents, but also makes it possible to update the prior fragility functions as more data becomes available. In this regard, the application of probability updating-adapting feature of the BN in light of newly available field data/observations (Khakzad et al., 2013) or hierarchical Bayesian analysis (Khakzad et al., 2014a,b) can also be considered as a viable alternative to handle data scarcity and perform probability updating from one hand and to combine dependent failure modes from the other hand. This will be the scope of our future work.

6. Conclusions

In this study we developed a methodology for vulnerability assessment of chemical installations, in particular aboveground storage tanks, subject to floods. The probabilities of individual failure modes such as floatation, buckling, and (impact-induced) sliding were estimated in form of fragility curves using logistic regression for which the required data was generated via limit state equations and Monte Carlo simulation. Although only large storage tanks were considered in this study, it was

illustrated that the floatation is the most prevailing failure mode, especially when the height of chemical inside a storage tank is roughly less than the height of flood inundation.

For buckling failure mode, the results of the present study show that the height of flood inundation seems to be a more influential parameter than the flow velocity as the shell buckling was observed merely for a high-water flood condition (i.e., floods with a height of inundation greater than 1 m). It is worth noting that in the present study the impact-induced buckling was not taken into account which might have increased the likelihood of shell buckling in case of high-flow floods. Regardless, it was demonstrated that the probability of buckling can significantly be lowered even with small amounts of containment (around 0.5m of crude oil in this study). As for sliding failure mode, none of regular floods (neither high-water nor high-flow flood condition) can seem to cause the storage tanks to slide; nevertheless, the sliding of tanks (if they have already not floated) due to the impact force of other floating tanks (also known as impact-induced sliding) is a credible failure mode which should not be overlooked. The results obtained in the present study regarding the relationship between the failure modes and the characteristics of floods and process vessels have been calculated under certain simplifying assumptions and need to be verified under a broader range of assumptions and test circumstances before being extended to other case studies.

In the present study we illustrated that due attention should be paid to dependencies when combining individual failure modes. The dependencies mainly arise due to common load-resistance parameters (e.g., common flood inundation height and velocity) contributing to several failure modes, from one hand, and conditional dependencies among the failure modes(e.g., those between floatation and sliding) from the other hand. We demonstrated that both types of such dependencies can effectively and transparently be taken into account in a Bayesian network methodology.

References

American Society of Civil Engineers (ASCE). Minimum Design Loads for Buildings and Other Structures. ASCE/SEI 7-05. Reston, Virginia. 2006. ISBN: 0-7844-083 1-9.

API Standard 620. Design and Construction of Large, Welded, Low-pressure Storage Tanks. 12th Edition. American Petroleum Institute Publishing Services, Washington. D.C. 2013.

API Standard 650. Welded Tanks for Oil Storage. 11th Edition. American Petroleum Institute Publishing Services, Washington. D.C. 2007.

Campedel M. Analysis of major industrial accidents triggered by natural events reported in the principal available chemical accident databases. European Commission Joint Research Centre. EUR-Scientific and Technical Research Report: JRC42281. OPOCE. 2008. ISSN: 1018-5593. Available online at http://publications.jrc.ec.europa.eu/repository/handle/JRC42281.

Cozzani V. Campedel M, Renni E, Krausmann E. Industrial accidents triggered by flood events: analysis of past accidents. Journal of Hazardous Materials, 2010; 175: 501-509.

Ebeling C. 2004. An Introduction to Reliability and Maintainability Engineering. Tata McGraw Hill, New Delhi. ISBN-13: 978-0-07-042138-7.

Federal Emergency Management Agency (FEMA).1995. Engineering principles and practices for retrofitting floodprone residential buildings. FEMA Rep. No. 259, Washington, D.C.

GeNie. Decision Systems Laboratory, University of Pittsburgh, GeNie, Version 2.0.5219.0, April2014, available online at: ⟨http://www.genie.sis.pitt.edu⟩.

Girgin S, Krausmann E. RAPID_N: Rapid natech risk assessment and mapping framework. Journal of Loss Prevention in the Process Industries, 2013; 26: 949-960.

Godoy LA. Performance of storage tanks in oil facilities damaged by Hurricanes Katrina and Rita. Journal of Performance of Constructed Facilities, 2007; 21(6): 441-449.

Haehnel RB, Daly SF. Maximum impact force of woody debris on floodplain structures. Journal of Hydraulic Engineering, 2004; 130(2): 112-120.

Hosmer D, Lemeshow S, Sturdivant R. 2013. Applied Logistic Regression. 3rd Edition. Wiley & Sons, Hoboken, New Jersey. ISBN: 978-0-470-58247-3.

Iturgaiz Elso M. Finite Element Method studies on the stability behavior of cylindrical shells under axial and radial uniform and non-uniform loads. 2012. Universidad Pública de Navarra, Spain. Available online at http://academica-e.unavarra.es/handle/2454/6186.

Kameshwar S, Padgett JE. Fragility assessment of above ground petroleum storage tanks under storm surge. 12th International Conference on Applications of Statistics and Probability in Civil Engineering, ICASP 12, Vancouver, Canada, July 12-15, 2015.

Khakzad N, Khan F, Amyotte P. Safety analysis in process facilities: Comparison of fault tree and Bayesian network approaches. Reliability Engineering and System Safety, 2011; 96: 925–932.

Khakzad N, Khan F, Amyotte P. Dynamic safety analysis of process systems by mapping bow-tie into Bayesian network. Process Safety and Environmental Protection, 2013; 91: 46–53.

Khakzad N, Khan F, Paltrinieri N. On the application of near accident data to risk analysis of major accidents. Reliability Engineering and System Safety, 2014a; 126: 116–125.

Khakzad N, Khakzad S, Khan F. Probabilistic risk assessment of major accidents: application to offshore blowouts in the Gulf of Mexico. Journal of Natural Hazards, 2014b; 74:1759–1771.

Khakzad N, Khan F, Amyotte P. Major accidents (Gray Swans) likelihood modeling using accident precursors and approximate reasoning. Risk Analysis, 2015; 35(7): 1336-1347.

Korkmaz K, Sari A, Carhoglu A. Seismic risk assessment of storage tanks in Turkish industrial facilities. Journal of Loss Prevention in the Process Industries, 2011;24: 314-320.

Krausmann E, Mushtaq F. A qualitative Natech damage scale for the impact of floods on selected industrial facilities. Natural Hazards, 2008; 46: 179–197.

Landucci G, Antonioni G, Tugnoli A, Cozzani V. Release of hazardous substances in flood events: damage model for atmospheric storage tanks. Reliability Engineering and System Safety, 2012; 106: 200-216.

Landucci G, Necci A, Antonioni G, Tugnoli A, Cozzani V. Release of hazardous substances in flood events: damage model for horizontal cylindrical vessels. Reliability Engineering and System Safety, 2014; 132: 125-145.

Mebarki A, Willot A, Jerez S, Reimeringer M, Prod' Homme G. Vulnerability and resilience under effects of tsunamis: case of industrial plants. Procedia Engineering, 2014; 84: 116-121.

Neapolitan R. 2003. Learning Bayesian networks. Upper Saddle River, NJ, USA: Prentice Hall, Inc.

Pearl J. 1988. Probabilistic reasoning in intelligent systems. San Francisco, CA: Morgan Kaufmann.

Region 6 Regional Response Team (RRT6). Flood Preparedness. Recommended Best Practices. Fact Sheet #103, January 2016. Available online at: http://www.deq.louisiana.gov/portal/portals/0/news/pdf/FloodPrepFactSheetDRAFT.pdf.

Salzano E, Iervolino I, Fabbrocino G. Seismic risk of atmospheric storage tanks in the framework of quantitative risk analysis. Journal of Loss Prevention in the Process Industries, 2003; 16: 403-409.

Santella N, Steinberg LJ, Sengul H. Petroleum and hazardous material releases from industrialfacilities associated with Hurricane Katrina. Risk Analysis, 2010; 30(4): 635-649.

Van Erp N, Van Gelder P. Bayesian logistic regression analysis. 32nd International Workshop on Bayesian Inference and Maximum Entropy Methods in Science and Engineering, Garching, Germany, 15-20 July 2012.

Van Gelder P. 2013. Flood Risk Management, Quantitative Methods, in Encyclopedia of Environmetrics, El-Shaarawi and Piegorsch (eds), John Wiley & Sons Ltd: Chichester, UK. DOI: 10.1002/9780470057339.

White F. Fluid Mechanics. 2003. 5th edition. McGraw-Hill, Boston. ISBN-13: 978-0072402179.

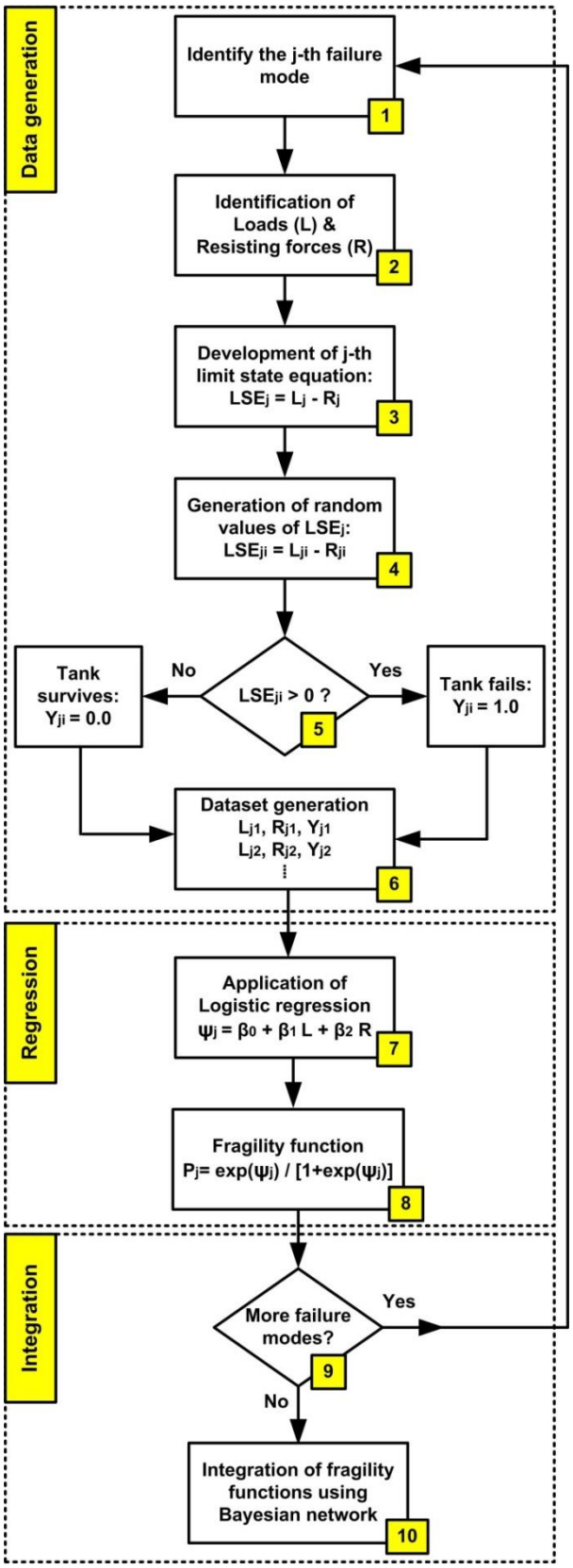

Figure 1. Schematic of the proposed methodology

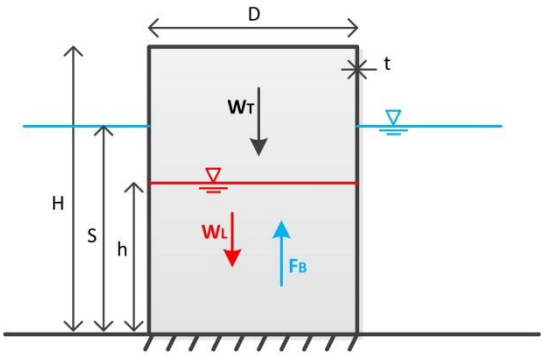

Figure 2. Schematic of the load-resistance forces considered for tank floatation.

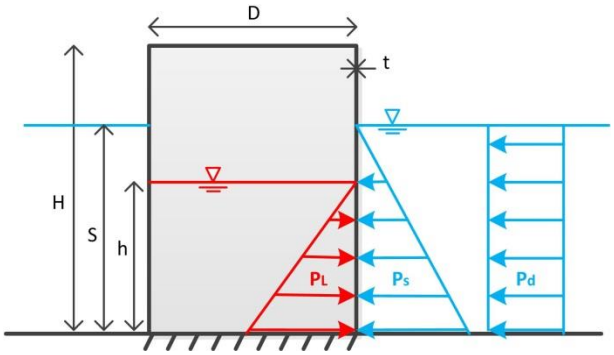

Figure 3. Schematic of the load-resistance forces considered for shell buckling.

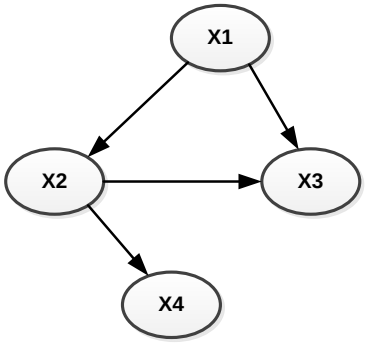

Figure 4. A typical Bayesian network.

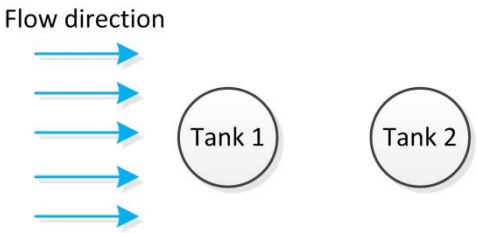

Figure 5. Schematic of the storage tanks exposed to flood.

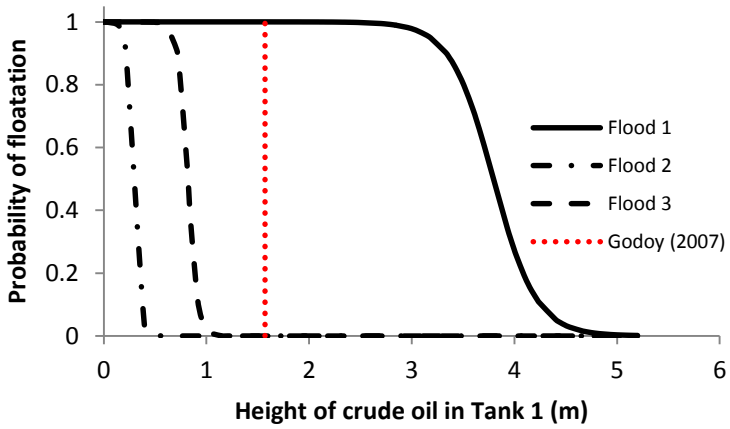

Figure 6. Fragility curves of Tank 1 due to floatation.

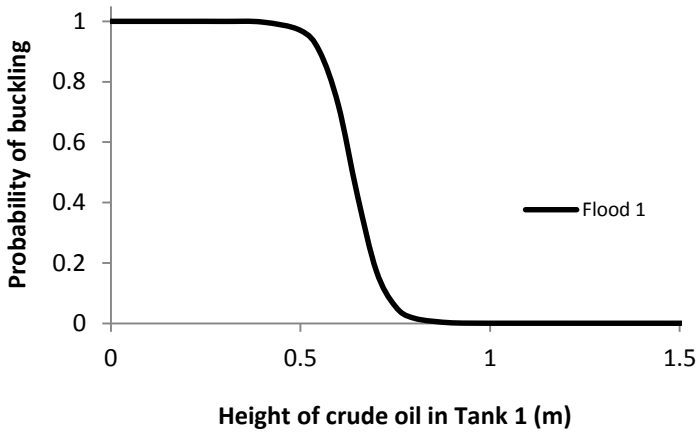

Figure 7. Fragility curves of Tank 1 due to shell buckling.

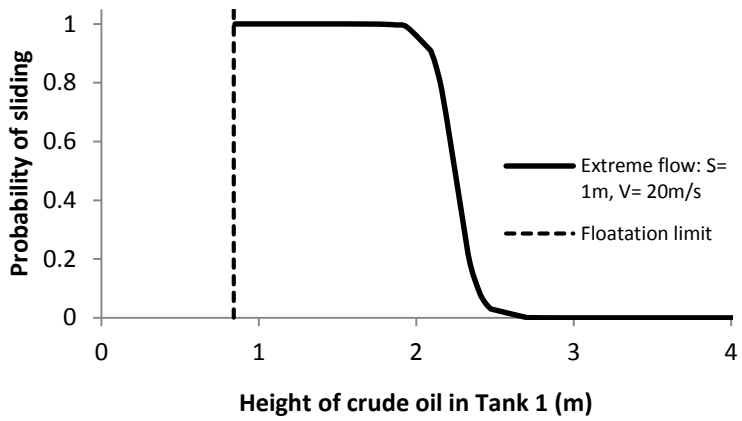

Figure 8. Fragility curve of Tank 1 due to sliding in case of an imaginary extreme flood.

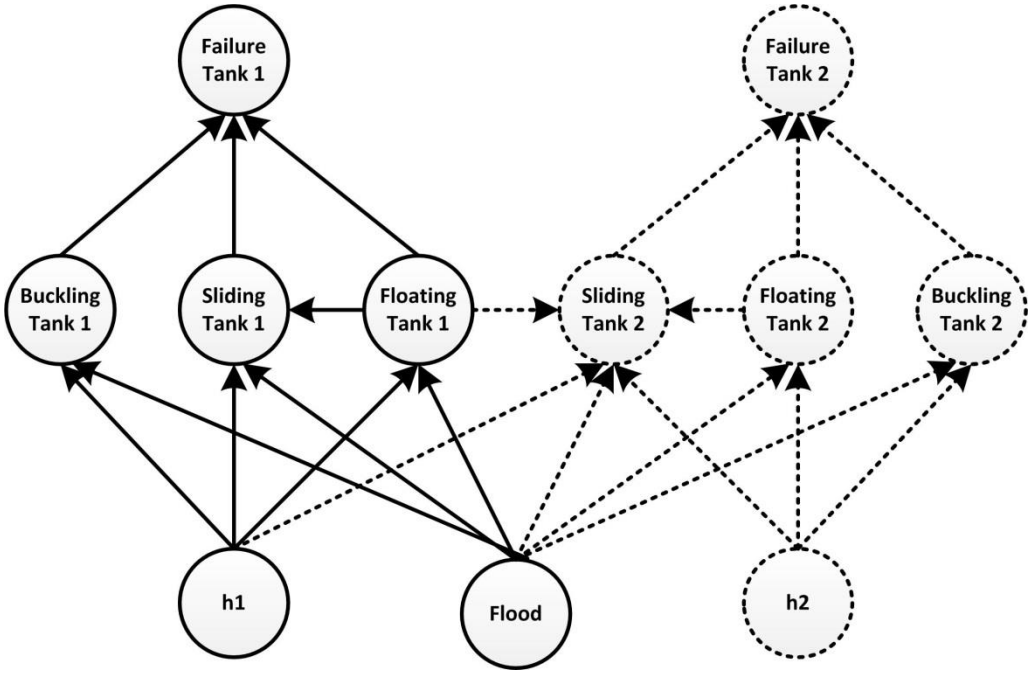

Figure 9. Bayesian network to combine failure modes.

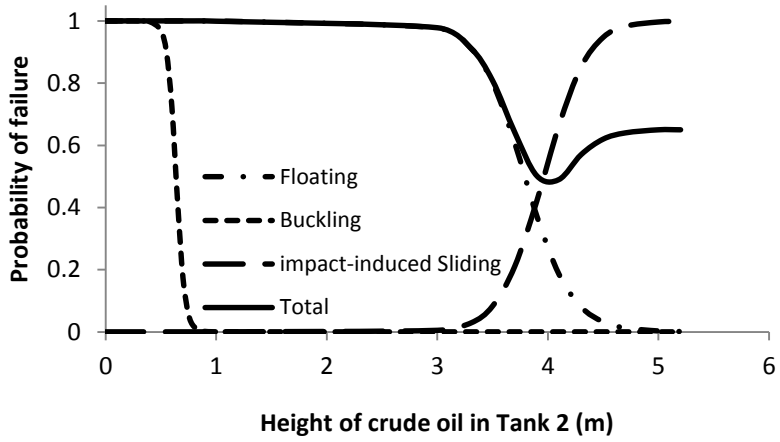

Figure 10. Fragility curves of Tank 2 due to individual and total failure modes. The probabilities of sliding have been averaged over different states h1.

Table 1. Numeric parameters used for the case study.

Parameter	Symbol	Value	Unit
Tank's height	H	6.1	m
Tank's diameter	D	91.5	m
Tank's shell thickness	t	0.015	m
Crude oil height	h	Uniform (0.0 , 5.2)	m
Flood's inundation height*	S	3.7, 0.5, 1.0	m
Flood's flow velocity*	V	0.25, 2.5, 1.0	m/s
Tank shell density (steel)	ρ_s	7900	kg/m^3
Flood water density	ρ_w	1024	kg/m^3
Crude oil density	ρ_l	900	kg/m^3
Young's modulus	E	2.1 E +11	Pa
Buckling critical pressure	P_{cr}	3.15 E +04	Pa
Impact duration	t_i	0.03	s
Poisson ratio	v	0.3	
Drag coefficient	C_d	1.8	
Friction coefficient	C_f	0.4	
Number of buckling waves	n	2	

* The numbers refer to Flood 1, Flood 2, and Flood 3, respectively.

Table 2. Optimal values of regression parameters β_0, β_1, and β_2 (the first, second, and third values in the table, respectively). For Tank 1: $\Psi(h1)=\beta_0+\beta_1 h1$ whereas for Tank 2: $\Psi(h1,h2)=\beta_0+\beta_1 h1+ \beta_2 h2$. NA: Not Applicable.

Tank 1	Flood 1	Flood 2	Flood 3
Floatation	18.16, -4.79	9.01, -31.17	17.5, -21.33
Buckling	16.06, -25.17	NA	NA
Sliding	NA	NA	NA
Tank 2			
Impact-induced sliding	-24.6, 0.49, 5.95	3.7, -17.55, 0.535	0.027, -0.7, 0.556